

# 1 Estimating human mobility in Holocene Western Eurasia with 2 large-scale ancient genomic data

3 Clemens Schmid & Stephan Schiffels\*

4 2021

## 5 **Significance Statement**

6 Ancient human DNA (aDNA) extracted from archaeological contexts (e.g. burials) allows to reconstruct  
7 past population movements. Relevant methods work by calculating proportions of shared ancestry among  
8 individuals or groups in order to answer specific, regional research questions. Here, we propose a large-  
9 scale algorithm to quantify human mobility through time and space using bulk aDNA data. The algorithm  
10 has two core components: i) Interpolation of the spatio-temporal distribution of genetic ancestry to obtain  
11 a continuous ancestry information field and ii) estimation of the spatial origin of each input sample by  
12 projecting its ancestry into this field. We apply this to thousands of published genomic samples in the last  
13 10,000 years to trace diachronic mobility patterns across Western Eurasia.

## 14 **Abstract**

15 The recent increase in openly available ancient human DNA samples allows for new, large-scale meta analysis  
16 applications. Trans-generational past human mobility is one of the key aspects that ancient genomics can  
17 contribute to, since changes in ancestry – unlike cultural changes seen in the archaeological record – neces-  
18 sarily reflect movements of people. Here we present a new algorithm to quantify past human mobility from  
19 large ancient genomic datasets. The key idea of the method is for each individual to compare a hypothetical  
20 genetic "origin" point with its actual burial point in space. This is achieved by first creating an interpolated  
21 ancestry field through space and time based on Multidimensional scaling and Gaussian process regression,  
22 and then using this field to map the ancient individuals into space according to their genetic profile. We apply  
23 this new algorithm to a dataset of 3191 aDNA samples with genome-wide data from Western Eurasia in the  
24 last 10,000 years and derive a diachronic measure of mobility for subregions in Western, Central, Southern  
25 and Eastern Europe. For regions and periods with sufficient data coverage, our mobility estimates show  
26 general concordance with previous results, but also reveal new signals of movements beyond the well-known  
27 key events.

---

\*Max Planck Institute for Evolutionary Anthropology (Deutscher Platz 6, 04103 Leipzig, Germany) and Max Planck Institute  
for the Science of Human History (Kahlaische Strasse 10, 07745 Jena, Germany) – Correspondence should be addressed to:  
stephan\_schiffels@eva.mpg.de

## 28 Introduction

29 All human behaviour is spatial behaviour and spatial perception and interaction is deeply rooted in the  
30 human mind. Individuals have *activity space* [Per+13] and need *personal space* [Høg08]. They interact with  
31 each other [ALB18] or the natural environment [Häg05] in space. And, finally, they create entirely new spatial  
32 environments [Boi+16]. Understanding movements in space – mobility – on different orders of magnitude  
33 is therefore a major component for understanding human behaviour throughout history [Bel14], from the  
34 Iceman’s lonely quest through the Ötztal Alps, to the Viking expansion even beyond Medieval Europe, and  
35 maybe eventually mankind’s escape to the stars.

36 Archaeological and anthropological theory provides different concepts and categories to classify mobility.  
37 Mobility can be a group property or individual behaviour and it has complex implications for the formation,  
38 perception and interaction of identity [Kel92; Ben01; LM15]. Migration, a special type of mobility perhaps  
39 to be defined archaeologically as the “*temporal and spatial collimation of a regional source of dispersed*  
40 *cultural property*” [Bur00], is an especially controversial topic [Ant90]. It is notoriously difficult to prove and  
41 to uncover its causes among the many interdependencies *micro-* and *macro theories* of migration suggest.  
42 Narratives of migration are also notoriously vulnerable to political instrumentalization [Wol19].

43 The field of archaeogenetics now provides a new perspective on past human mobility and migration, which  
44 is at its very core influenced by population genetics theory. The emergence, change and distribution of human  
45 ancestry components – mediated by the mobility of their hosts – is in fact one of its most important research  
46 questions (e.g. [Haa+15; Lip+18; Fle+19]), causing fruitful and corrective friction with the humanities [Fur18;  
47 GF20; Fur21]. While so far much archaeogenetic research focuses on particular cultural-historical contexts,  
48 the recent growth of published ancient DNA samples from all around the world enables a new category of  
49 quantitative meta analysis.

50 Large, explicitly spatiotemporal datasets have been part of population genetics research for a long time  
51 already [BR19], sometimes even with a focus on mobility quantification [PNS15; BRC16; Al+19; PPN19].  
52 But to our knowledge up to the time of this writing, only few attempts have been made to systematically  
53 derive a continuous, large-scale and diachronic measure of human mobility with ancient genetic data. These  
54 are most notably a pioneering publication by Loog et al. 2017 [Loo+17] and another approach by Racimo  
55 et al. 2020 [Rac+20]. Loog et al. measure mobility in prehistoric Europe by comparing the distance matrix  
56 correlation among spatial, temporal and genetic distance for aDNA samples in moving 4000 year windows. As  
57 a result they generate an unscaled mobility proxy curve that indicates elevated levels of mobility correlating  
58 to the Neolithic expansion, the Steppe migration and finally the European Iron Age. Racimo et al., on  
59 the other hand, employ admixture analysis to individually attribute genomic samples a genetic profile with  
60 respect to three specific ancestry components: Mesolithic hunter-gatherers, Neolithic farmers with ancestry  
61 originating in the Near East, and Yamnaya steppe herders, arriving in Europe during the third millennium  
62 BC. They derive mobility as a wave front speed of surpassed ancestry component thresholds. To overcome  
63 sample sparsity and to correlate the arrival of certain ancestry components with biogeographic metrics, they  
64 use Gaussian process regression for the interpolation of relative ancestry component occurrence – an idea we  
65 also took as a starting point for our proposed mobility estimation method.

66 In this paper we present a new algorithm (Fig. 1) to estimate past human mobility on the individual  
67 level. For each individual it determines multiple spatiotemporal positions of close genetic affinity, which, as  
68 we show, can often be interpreted as ancestral origin points. The distance between the location where an  
69 individual was buried and these points serves as a proxy for personal mobility in an individual’s (or their  
70 immediate ancestors’) lifetimes. We apply this algorithm to several thousand previously published ancient

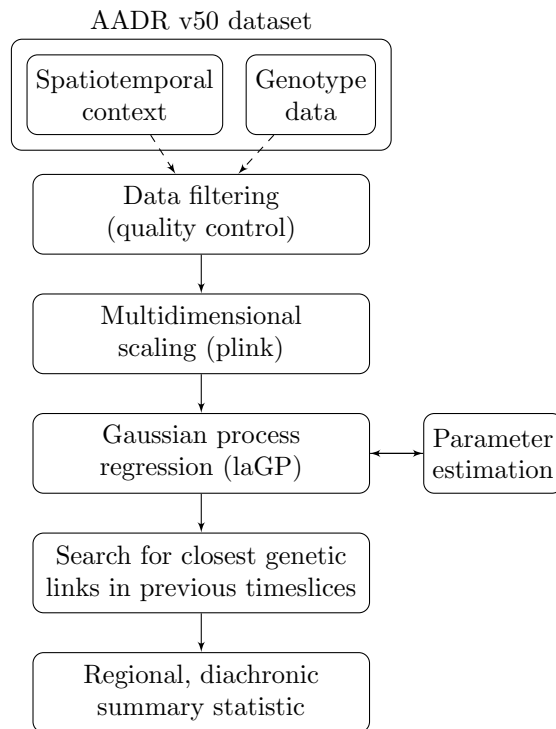


Figure 1: Schematic overview of the general workflow.

71 genomes from Western Eurasia dating from between 8000BC and 2000AD (excluding modern genomes) taken  
72 from the Allen Ancient DNA Resource (AADR) [Dav21]. And we show that, while the average results largely  
73 match expectations including known and large-scale movements at the beginning and end of the Neolithic,  
74 these large-scale patterns are accompanied by considerable individual-level heterogeneity.

## 75 Results

### 76 Interpolating genetic ancestry through space and time

77 A key challenge for understanding shifts of ancestry through space and time is the inherent sparsity of  
78 archaeological data. To counter this we employed an interpolation technique fitted upon 3191 published  
79 samples from 85 publications currently available in the AADR [Dav21] for Western Eurasia during the  
80 Holocene. All samples in this public data collection reference single-nucleotide polymorphisms (SNPs) from  
81 a panel of about 1.24 million known informative positions [Mat+15] and our dataset is filtered according to  
82 general sample quality criteria (see Methods). Within the derived subset, the data distribution in time and  
83 space is heterogeneous (Fig. 2), with generally few data points from the European Mesolithic, significantly  
84 more from the Neolithic, then most from the Bronze Age and again less from the Iron Age and later periods.  
85 The diachronic amount of data from Great Britain, Iberia, Central Europe and Southeastern Europe is  
86 comparatively high, whereas other regions are less well covered.

87 We applied multidimensional scaling (MDS) on this data to reduce its dimensionality to two summarising  
88 ancestry components (Fig. 3), that are by construction most informative about the genetic diversity across  
89 the sample set (see Supplementary Text 3.1 and Supp. Fig. 7 for a run with three result dimensions). We find

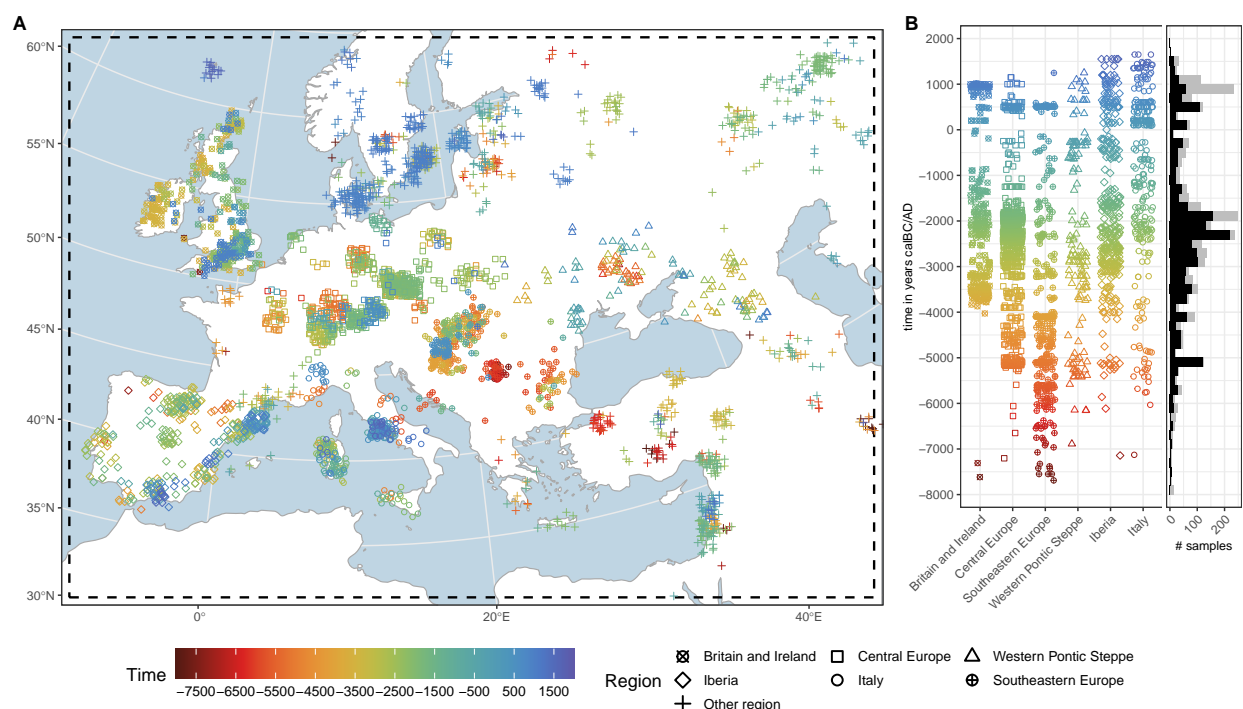


Figure 2: Spatial and temporal distribution of the aDNA sample selection. **A**: Map (EPSG:3035, ETRS89 Lambert Azimuthal Equal-Area, "European grid") with the research area (dashed). Samples are jittered with up to  $\pm 60$ km in x and y direction to reduce the effect of overplotting. The sample dots are coloured according to their temporal origin, where the time is given in years calBC/AD (negative values indicate ages calBC). The sample dot shape encodes the attribution to different analysis regions. **B**: Scatter plot of temporal sample distribution for each analysis region. The stacked histogram on the right shows the sample count through time for all samples in grey, and for the ones within the defined analysis regions in black (bin width = 200 years).

90 the largest internal separation of samples to be along the tempo-cultural boundary between the Mesolithic  
 91 and the Neolithic, highlighting the strong population shift the Neolithic introduced into Europe [Laz+14;  
 92 Haa+10; Sko+12]. Many other patterns seen in the MDS are also consistent with previous observations and  
 93 will be discussed among our results below.

94 We modelled these two MDS-derived ancestry components individually as the dependent variable in a  
 95 Gaussian process regression (GPR) model with three independent input variables describing the position  
 96 of each sample in space and time. To learn the properties of the relevant covariance matrix ("*kernel*")  
 97 for a model with the best mean postdiction abilities we explored multiple methods: Variogram analysis,  
 98 maximum likelihood estimation and cross-validation (see Supplementary Text 1). With the parameterized  
 99 Gaussian process regression model we predicted iterations of average spatio-temporal genetic ancestry grids  
 100 across Europe (e.g. Fig. 4), explicitly sampling from the the temporal uncertainty of the input data.

101 The interpolation of ancestry components across time and space reflects how 10 millennia of human  
 102 population changes have shaped genetic ancestry in this area. As already seen in Fig. 3, both ancestry  
 103 components C1 and C2 here most strongly reflect the enormous changes that underlay the transitions during  
 104 the Early Neolithic, with increasing values (for C1 coloured in yellow in Fig. 4) throughout Central and  
 105 Western Europe around 5000BC as a result of people moving north-westwards from the Levant and western  
 106 Anatolia. They also prominently feature further changes after 3000BC, bringing ancestry previously located

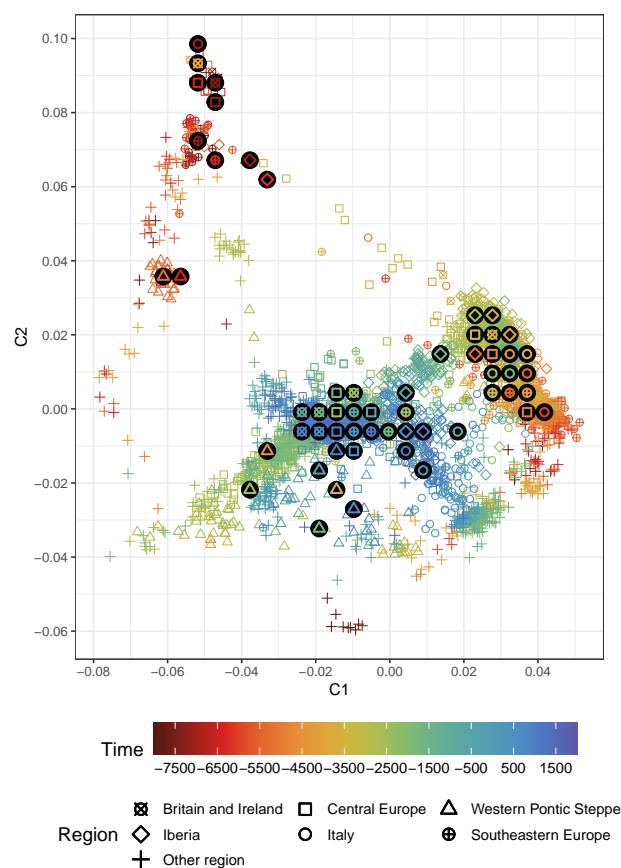


Figure 3: Scatter plot of the sample distribution in 2D multidimensional scaling space. Each sample is plotted with the same shape and colour as in Fig. 2. The bigger, black circles are the centroids of region-time groups (bin width = 1000 years). To prevent overplotting, the centroids are not printed on their exact positions, but instead rearranged in a non-overlapping lattice. See Supp. Fig. 7 for a 3D version and Supp. Fig. 8 for a larger version where the individuals mentioned in the text are highlighted.

107 in Eastern Europe and the Eurasian steppes into Western and Central Europe.

108 With this interpolation one can attempt the reconstruction of continuous, local ancestry histories even  
109 for places without consistent data coverage. To illustrate this, we selected arbitrary spatial positions (corre-  
110 sponding to six capital cities) and used the GPR model to postdict how the genetic profile in these locations  
111 changed through time (Supp. Fig. 4). The six "virtual" time-series again generally reflect our knowledge of  
112 the genetic changes in Europe: In London, Budapest, Rome and Barcelona we observe an ancestry shift with  
113 the arrival of Neolithic, and then once more with Steppe ancestry – with small regional differences. Riga, on  
114 the other hand, starts out with a higher degree of Eastern Hunter-Gatherer (EHG) ancestry before skipping  
115 the influx of the Anatolian farmer component. Jerusalem, expectedly, fills a markedly different spot on the  
116 genetic map.

### 117 Estimating individual-based mobility

118 While the interpolated ancestry field reflects the *average* change in ancestry through space and time, it  
119 also forms the basis for our proposed algorithm to understand *individual*-based mobility. The key idea is  
120 to assign to each individual a hypothesised place of closest genetic affiliation in a previous field timeslice

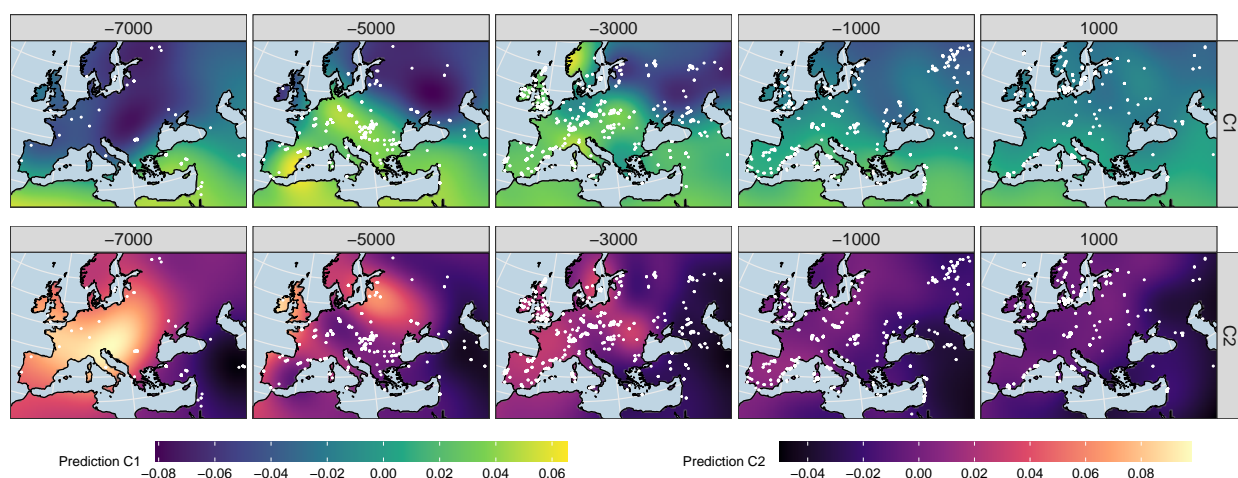


Figure 4: Gaussian process regression interpolation map matrix based on the multidimensional scaling dimensions (resolution: 50km). The five maps on top show timeslices through the interpolated, spatio-temporal 3D space for the derived ancestry component C1, the five on the bottom for C2. The samples from a time window  $\pm 1000$  years around the slicing position are plotted as white dots.

121 (i.e. multiple hundred years before said individual), which we interpret as point of ancestral origin. The  
122 difference of this ancestral origin point and the factual burial position is a quantitative measure of ancestry  
123 relocation through inter- or intragenerational mobility. As an example, consider an individual from Roman-  
124 time Britain (individual 3DRIF-26 from ref. [Mar+16]), buried in York, but featuring a genetic ancestry  
125 profile from the Near East. This is a clear case where the authors concluded that either this individual  
126 themselves or their ancestors came from the Near East, but ended up in Britain. In this case, we would thus  
127 infer an "origin- or mobility vector" pointing from Britain to the hypothesised region in the Levant, resulting  
128 in an origin-distance of several thousand kilometres and in south-western direction (Fig. 5C).

129 It is indeed instructive to consider our approach with other well understood individuals that represent  
130 outliers in their genetic signatures, and which have been used in the past to illustrate mobility. Figure 5  
131 shows four such concrete cases for specific published samples. The individual named Stuttgart, one of the  
132 first ancient genomes sequenced [Laz+14], is also one of the earliest Neolithic samples from Central Europe.  
133 They display non-local genetic ancestry in the sense that they differ strongly from preceding Mesolithic  
134 samples in the area. In our analysis, we show that indeed the lowest genetic distances for this individual  
135 can be found in Anatolia and Southeastern Europe (Fig. 5A). This indicates mobility from there to Central  
136 Europe in accordance with archaeological models [Por+20]. The lowest genetic distances can be observed  
137 to Southern Europe, where the Neolithic expansion followed another route [Boc+09; Boc+12]. In the late  
138 Neolithic, individuals affiliated with the Corded Ware culture from Central Europe have been identified as  
139 one of the earliest with so-called Steppe ancestry, which was present already before 3000BC in the Pontic  
140 Caspian steppe. Indeed, for a representative sample from that group (RISE434), we find the closest matching  
141 ancestry points falling into Eastern Europe (Fig. 5B). Finally, confirming the analysis by Haber et al. 2019  
142 [Hab+19], we find that multiple samples (for example SI-40) extracted from a mass burial near a Crusader  
143 castle in Sidon in present-day Lebanon are linked to Iberian ancestry profiles (before the Umayyad conquest)  
144 (Fig. 5D).

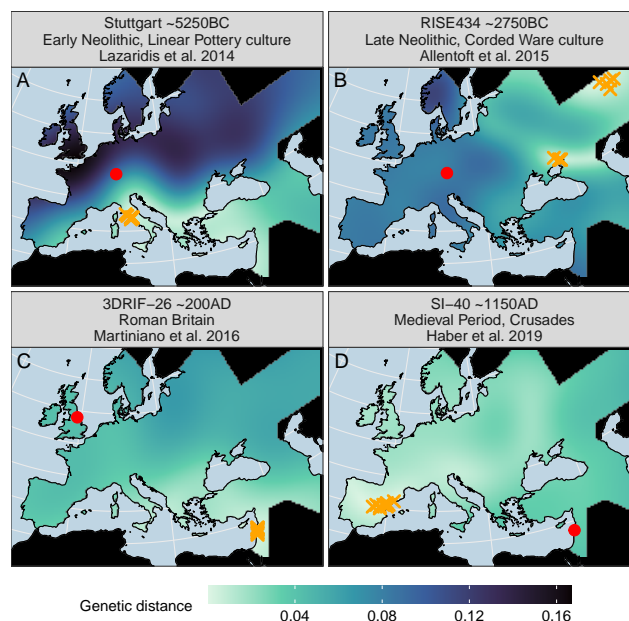


Figure 5: Genetic distance map matrix for four selected individuals. The red dots show their burial position. For each individual ten temporal re-sampling iterations of prediction grids (resolution: 30km) for C1 and C2 were created, where each grid is a timeslices several hundred years before the median burial age – just as for the slices in Figure 4. For these timeslices the genetic distances (Euclidean distance in 2D MDS space) between the individual and each field grid point were calculated, thus creating a smooth raster indicating regions with increased or decreased genetic similarity to the respective individual. The orange crosses mark the ten points of minimal genetic distance.

## 145 Regional mobility patterns during the last 10,000 years in Western Eurasia

146 Given our interpolation model for the average ancestry through space and time, and the individual-based  
147 mobility as computed using the origin search algorithm described above, we can derive a mobility-vector for  
148 every single sample in our dataset and investigate these vectors through time. The results of that analysis  
149 are summarised in Figure 6, both in terms of the lengths of individual mobility vectors (shown on the y-axis)  
150 and direction (shown in colour according to the legend). While in principle we can apply our algorithm to  
151 every sample in the dataset, we here focus on a selection of confined regions with acceptable coverage of  
152 samples throughout the study time period (Fig. 2). We mostly consider patterns emerging from long-distance  
153 signals, observed as individual points with large origin-distances (typically 1000km and further), as these  
154 typically correspond to events described previously in the literature and thereby provide a proof-of-concept  
155 for our method. However, beyond these long-distance signals, we highlight a considerable level of complexity  
156 of smaller-scale signals that may correspond to previously unknown events. Shown along the individual  
157 distances is a moving average curve together with an error band (in grey shading), which in some cases may  
158 help putting the largest individual-based events into context. Alternative visualizations of the time series  
159 shown in Figure 6 are available with the Supplementary Figures 5 and 6.

160 Beginning with our time series from Great Britain and Ireland, the largest observed individual signals  
161 correspond to the Early Neolithic in the 4th millennium BC [She10; Tho15; Bra+19; Sán+19a; Cas+20],  
162 the Bell-Beaker transition after around 2500BC [Cas+16; Ola+18], Roman Britain and the Viking pe-  
163 riod [Mar+20b]. Note for example the indicative individuals I6747 [Bra+19], I5367 [Ola+18], 3DRIF-26

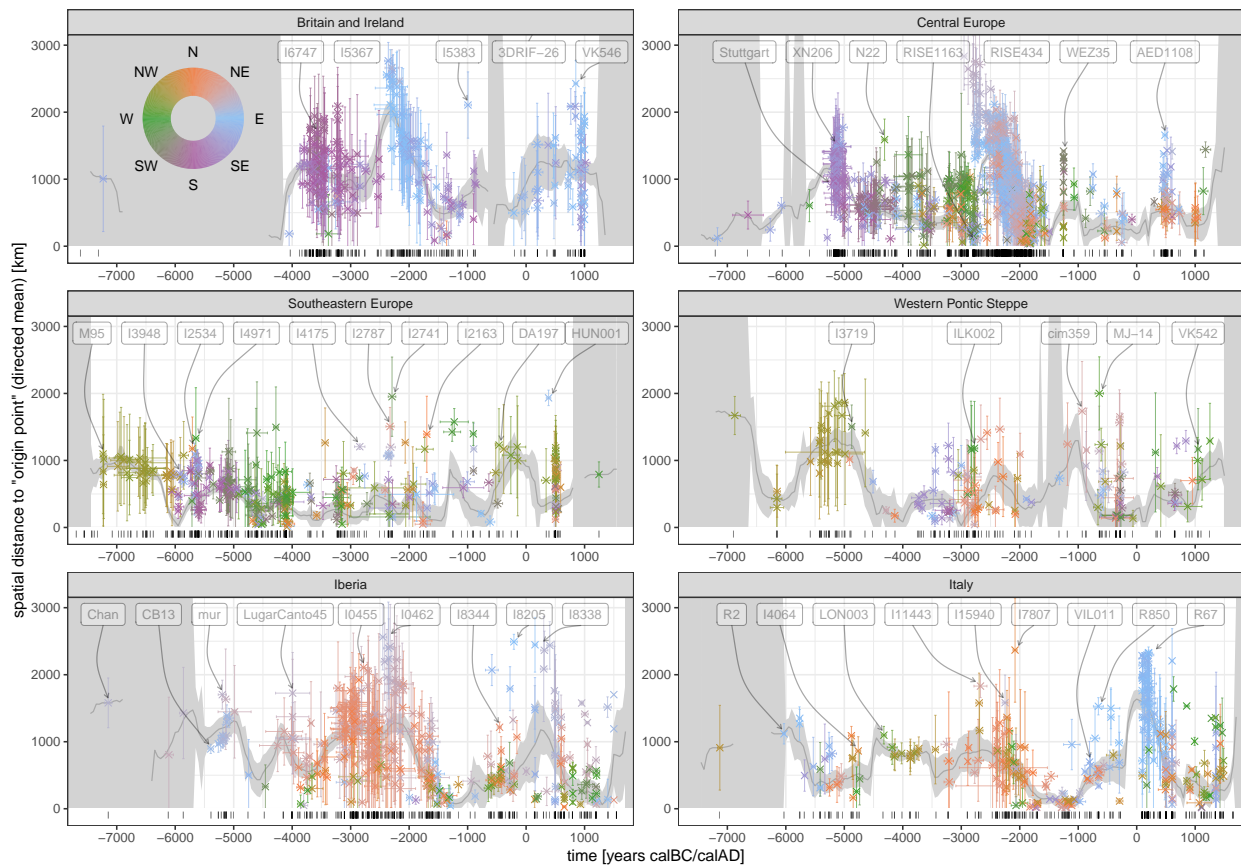


Figure 6: Mobility estimation results. One scatter plot for each of the six analysis regions (see Fig. 2). Each dot represents the mean mobility vector for one sample across 100 temporal re-sampling runs. The position on the x-axis is the mean of the sampled ages in years calBC/AD, and the position on the y-axis is the mean distance to the 100 origin points, with dot colour encoding the mean direction according to the circular legend in the top-left corner. Each observation comes with error bars on the x- and y-axis, covering one standard deviation of the 100 resampling observations. The distance mean per observation is a directional mean, so opposing vectors cancel each other out, whereas the standard error is calculated from absolute distances. The barcode plot at the bottom of each subplot documents the diachronic data coverage for each region. The smooth grey curve printed below the samples is a 400 year moving mean for the spatial distance. It is calculated from the total set of the 100 resampling iterations. The dark grey ribbon accommodating this mean curve, on the other hand, is the standard error of the mean based on the mean dots displayed here. It is visualized as infinite if a given 400 year time window has less than three observation.

164 (>3000km; already discussed above) [Mar+16] and VK546 [Mar+20b], which each represent extremely long  
 165 distance mobility. Direction-wise, the respective mobility peaks are consistent with what we know about the  
 166 sources for these events, with Southern sources during the Neolithic, and Eastern sources during the Bell-  
 167 Beaker and Viking periods. The Neolithic transition is visible in our mobility proxy as a clear upwards-jump,  
 168 both in the average and individual origin distances, contrasting the few sufficiently well covered and appar-  
 169 ently very "local" Mesolithic individuals from before 4000BC. But this peak only dies down surprisingly  
 170 slowly until the first half of the third millennium, attributing almost every Neolithic individual a foreign  
 171 "origin". To some degree this might be an effect of the smooth, only slowly recoiling ancestry interpolation  
 172 model and the peripheral position of Britain and Ireland, which renders origin positions on the continent  
 173 disproportionately likely. But the tardiness of the recovery also supports the assumption of a large and stable



174 sphere of interaction or at least strong genetic similarity across Western Europe during the Neolithic. We  
175 will discuss a corresponding observation below for Central Europe and Iberia. The following Bronze Age  
176 peak, triggered by incoming ancestry ultimately from Eastern Europe, is remarkably strong (see also Supp.  
177 Fig. 6) and persists even after the initial Bell-Beaker transition. For the period after 2000BC Olalde et al.  
178 2018 suggest a much more homogeneous gene pool, which does not rule out the possibility of "incoming con-  
179 tinental populations with higher proportions of Neolithic-related ancestry" [Ola+18], though. These might  
180 be one reason for the mobility vectors pointing to the East and South in the Middle Bronze Age. In the  
181 Late Bronze Age the individual I5383 [Ola+18] stands out with a long mobility vector pointing to Eastern  
182 Europe. As they are not separated from their contemporary peers in MDS space (Supp. Fig. 8), we assume  
183 their outlier position to appear incorrectly inflated here.

184 For Central Europe we observe similar peaks as for Britain and Ireland. The Neolithic expansion reaches  
185 this area in the late sixth millennium and leads to a first, strong uptick of the mobility signal from the  
186 Southeast [GD15; Lip+17; Nik+19; Bru+20], visible for example in the aforementioned Stuttgart individual  
187 [Laz+14] or XN206 from Stuttgart-Mühlhausen [Riv+20]. These individuals' origin points cover a wide  
188 corridor from Western Anatolia to the Balkans, with some directed also towards the Southern route of the  
189 Neolithic in Italy. Not unlike the post-Neolithisation development in Britain, the mobility pulse then dies  
190 down only slowly in the fifth millennium. An interesting case in this spatiotemporal context is individual  
191 N22 from modern day Poland. Fernandes et al. 2018 [Fer+18] describe them as "the most recent individual  
192 ( $\approx$ 4300 BCE) with a complete genomic WHG attribution to be found to date in an area occupied by Danubian  
193 Neolithic farmers", which causes our origin search to link them to remaining hunter-gatherer populations  
194 i. a. in Ireland. In the first half of the third millennium Steppe ancestry arrives, as observed in many Late  
195 Neolithic Corded Ware individuals – like aforementioned RISE434 [All+15]. Their origin vectors then clearly  
196 point into the far East and Northeast [Haa+15; All+15; Bru+20; Fur+20; Lin+20]. This strong signal,  
197 lasting well into the Bronze Age, is heterogeneous both in distance and directionality. We caution that the  
198 spread of Steppe ancestry did most likely not follow a perfect wave-of-advance-like pattern, leaving pockets  
199 of unaffected or only later-affected ancestry behind, which will inevitably result in more erratic mobility  
200 estimates. After 1500BC the data density for Central Europe decreases and general observations become  
201 more difficult. Given archaeological and eventually historical evidence, it is of course not unreasonable to  
202 assume a high degree of mobility in the Late Bronze Age, the Iron Age [KL05], and the Medieval period,  
203 connecting Central Europe to France, Great Britain, Southern Scandinavia, Eastern Europe and the Balkans,  
204 catalysed by different cultural processes [Ola+18; Mit+19]. Two remarkable individuals with long mobility  
205 vectors are WEZ35, which is representative for the relatively unstructured population documented from the  
206 Tollense Bronze Age battlefield in northern Germany [Bur+20], and AED1108 from Bavaria with strong  
207 skull deformation and about 20% East Asian ancestry [Vee+18].

208 Southeastern Europe stands out in our analysis, because we could include a high number of comparatively  
209 early samples from the Mesolithic, e.g. M95 [Gon+17]. All of them are from the small and extraordinary  
210 Iron Gates area in Serbia and Romania, where the Danube passes between the Balkan Mountains and the  
211 Southern Carpathian Mountains range. They therefore may not be representative for the entire region and  
212 their long mobility vectors pointing to the Northwest are probably an artefact of the also low data density  
213 in Central Europe and Britain, where our ancestry field misrepresents a most likely more Western Hunter-  
214 Gatherer-related (WHG) profile. During the 6th millennium BC, correlating well with the beginning of the  
215 Neolithisation in the region [Por+20], we observe more plausible non-locality signals: The ancestry profile  
216 of Early Neolithic individuals like e.g. I3948 [Mat+18] from the Adriatic coast, points, to Western Anatolia.

217 Surprisingly, for the individuals I2534 and I4971 [Mat+18; Lip+17], we observe a large origin distance to the  
218 North and West, even after the onset of the Neolithic. These individuals might not have been (personally or  
219 through his immediate ancestors) part of any permanent long-range mobility: they lived at a time and place  
220 where new ancestry was arriving with the Neolithic package – rapidly changing the local ancestry landscape  
221 – and their genetic “displacement” thus becomes an indirect proxy of the major mobility event surrounding  
222 them. I4971 even features some “first European farmers” (FEF) ancestry [Lip+17], which positions them  
223 between a local hunter-gatherer and the new farmer profile (Supp. Fig. 8). Unlike other European regions, the  
224 arrival of Steppe ancestry in Southeastern Europe appears more gradual, beginning earlier and less abruptly  
225 [Mat+18]. Few individuals show a clear mobility signal pointing to the far Northeast – e.g. I4175 [Mat+18].  
226 For later periods, finally, we observe some remarkable outliers with strong mobility signals: For example  
227 the Hungarian Bell Beaker individuals I2787 and I2741 [Ola+18], the Middle Bronze Age individual I2163  
228 from Bulgaria [Mat+18], the Iron Age Scythian DA197 [Bar+18] or the Migration Period Hunnic individual  
229 HUN001 [Gne+21].

230 Even further to the East, in the Western Pontic steppe (including the area north of the Greater Cau-  
231 casus mountain range), we see a quite varied account of ancestry influx. For the Ukrainian individuals  
232 from the sixth millennium and before, Mathieson et al. 2018 [Mat+18] report ancestry on a cline between  
233 Eastern-, Scandinavian Mesolithic- and later Western Hunter-Gatherers. This genetic affinity is reflected in  
234 the first increase of signal we observe mainly from the Northwest during the sixth millennium, confirming  
235 previously described similarities in the developments in Eastern and Northeastern Europe [Jon+17]. Only  
236 at the beginning of the fifth millennium one extraordinary Individual (I3719) stands out with “entirely  
237 northwestern-Anatolian-Neolithic-related ancestry” [Mat+18] and thus long-distance affinity to the West  
238 and Southwest. Most data for the Neolithic and the Bronze Age is from the Caucasus region and documents  
239 a complex, though relatively local mobility history [Wan+19]. Within this time frame, multiple Globular  
240 Amphora context individuals (e.g. ILK002 [Mat+18]) from present-day Ukraine stand out with a strong  
241 origin signal from the West. During the Iron Age, more individuals with a relatively long-distance mobility  
242 signal appear, most notably cim359 [Krz+18] and MJ-14 [Jär+19]. Their origin vectors point to the opposite  
243 ends of Europe, illustrating the region’s position as a bridge between Europe and Central Eurasia housing  
244 different equestrian steppe nomad populations – e.g. Cimmerians, Scythians, and Sarmatians (see also Supp.  
245 Fig. 5). This generally holds true into historical times, including the Migration- [Bar+18] and Medieval  
246 Periods (e.g. VK542 [Mar+20b]).

247 Already the first hunter-gatherer individual available from Iberia – Chan [Gon+17] – has a very large  
248 mean mobility vector. This signal is not reliable, though, given the fact that no local, preceding reference  
249 data exists, which could inform the ancestry field for the origin search to appreciable accuracy. Much more  
250 relevant are the observations for Early Neolithic individuals like CB13 [Ola+15] or mur [Val+18]. They  
251 document the southern route of the Neolithic expansion. From the second half of the fifth millennium to the  
252 middle of the third millennium many individuals from Iberia are attributed long origin vectors towards the  
253 North and Northeast (e.g. LugarCanto45 [Mar+17] or I0455 [Ola+18]), although others have described this  
254 period as a time of relative genetic stability [Ola+19]. This forms a parallel observation to Southern- and  
255 Western-facing origin vectors described above for Great Britain, Ireland and Central Europe between 4000  
256 and 2500BC. We suspect that this crisscrossing of origin vectors may be caused by the low levels of genetic  
257 differentiation among different Neolithic populations. The Neolithic expansion and the following resurgence  
258 of hunter-gatherer ancestry in populations in Iberia, Central Europe and Great Britain might have created  
259 a large geographic area of very similar genetic ancestry (see also Fig. 3). Alternatively – or additionally

260 – the Atlantic sphere of influence connecting Western European megalithic cultures (to be taken up later  
261 in the Bell Beaker phenomenon and beyond) could have indeed induced a high degree of mobility in said  
262 region [Tho15; Pau19; Sán+19b]. More clearly interpretable signals emerge later in the third millennium in  
263 Iberia with the arrival of Steppe ancestry – well visible through origin vectors pointing to the far Northeast  
264 for individuals like I0462 [Ola+18]. In the Iron Age and later we observe some non-locality from the North  
265 (e.g. I8344 [Ola+19]) – which could potentially be connected to the spread of Celtic languages to the region  
266 [Fis+18] – but then mostly from the East (e.g. I8205 and I8338 [Ola+19]), possibly through Greek and  
267 Roman influence. We note that the relative lack of samples from Northern Africa forced us to mostly exclude  
268 it from the genetic similarity search in our analysis, which masks all potential mobility that might have taken  
269 place between Europe and Africa [Gon+19].

270 The final focal region studied here, Italy, comprises not only the Italian Peninsula, but also Sicily and  
271 Sardinia. These go through partially independent developments not comprehensively represented in the  
272 available data. Samples from the sixth millennium are limited to Sicily as well as Northern and Central Italy.  
273 They fit well to what we know about the southern route of the Neolithic Expansion with ancestry arriving  
274 from the East [Ant+19]. Indeed, the ancestry vectors of Early Neolithic samples like R2 [Ant+19] point  
275 directly to Western Anatolia. A few hundred years later the Neolithic ancestry profile is distributed across  
276 large parts of Europe and our derived mobility proxy reflects less a point of origin for the respective Neolithic  
277 samples, but rather their entanglement in the preceding cross-European mobility phenomenon. We assume  
278 this to be the reason for the moderately strong mobility signal we measure from the the fifth to the middle of  
279 the fourth millennium (e.g. I4064 [Fer+20] and LON003 [Mar+20a]), arising despite almost all our input data  
280 is from Sardinia, where others have observed genetic continuity until the first millennium BC [Mar+20a].  
281 In the third millennium Steppe ancestry arrived on the Italian peninsula, heralding multiple long-distance  
282 mobility signals: The affected Sicilian and mainland individuals show affinity to the North and East – most  
283 notably I11443 [Fer+20] from Sicily, which was reported to have the highest amount of Steppe ancestry in ref.  
284 [Fer+20]. An even more extreme outlier, I7807, who has no Steppe ancestry, is misplaced by our algorithm,  
285 likely because absence of Steppe ancestry is rare at this late time in Europe. Their genetic profile thus lacks  
286 sufficient spatial support in our model and our search gets pushed towards the fringe of our analysis region.  
287 Note the Chalcolithic sample I15940 [Fer+20] from Sardinia with their eastern mobility signal. Fernandes  
288 et al. 2020 identified them as an outlier with ”significant affinity to Levantine and North African Neolithic  
289 individuals”. The second millennium in our Italy timeseries is almost exclusively covered by samples from  
290 Sardinia and Sicily, with a low mobility proxy signalling genetic isolation. During the Iron Age, Sardinia and  
291 the Italian mainland become once more part of an exuberant Mediterranean mobility network, as shown for  
292 example by the relatively long mobility vectors for VIL011 from a Carthaginian/Phoenician-Punic context  
293 [Mar+20a] or R850 [Ant+19], which Antonio et al. 2019 could model as a ”mixture between local people and  
294 an ancient Near Eastern population (best approximated by Bronze Age Armenian or Iron Age Anatolian  
295 [...])”. Given North-Africa was excluded from the origin search, many signal from this time period are not  
296 entirely reliable and miss an important ancestry component. We finally observe the most extreme signals  
297 of non-locality in Italy during the height of the Roman empire, in the first centuries AD, where a unique  
298 pattern of mostly Eastern non-local origin emerges, consistent with strong Near Eastern influx into the city  
299 of Rome (visible e.g. with individuals like R67 [Ant+19]).

## 300 Discussion

301 The method to estimate human mobility from genetic data we presented here is based on a simple key  
302 principle: Changes in genetic profiles are informative about population movements. This key principle is not  
303 new, and in fact is the core assumption behind all major archaeogenetic studies that have revealed mobility in  
304 the past. Most notably in Western Eurasia movements associated with the Neolithic expansion (e.g. [Haa+10;  
305 Sko+12; Ola+15; Lip+17; Fer+18; Fre+18; Bra+19; Nik+19; Riv+20]) and the arrival of Steppe ancestry  
306 (e.g. [All+15; Haa+15; Cas+16; Ola+18; Mit+19; Fer+20; Fur+20; Lin+20]). In our algorithm, we have used  
307 this basic principle to derive mobility at an individual level, by interpreting genetic profiles as quantitative  
308 proxies for a biogeographic field. A key challenge is the fact that the nature of this genetic-spatial mapping  
309 changes through time, due to human movement, the very subject of this study. Conceptually, there can never  
310 be a perfect solution to this challenge, since ultimately genetic ancestry is *not* tied to geographic space, but  
311 to mobile people living in this space. In our method, we have addressed this by using Gaussian process  
312 regression to approximate an *average* ancestry field, which is by construction forced to change only slowly  
313 through space and time. It thereby forms the basis to determine individual-wise mobility as differences in  
314 relation to the slower group-based shifts in ancestry. These choices result in individual and average mobility  
315 signals which generally fit the published state of research as reconstructed from the very same samples. The  
316 Neolithic demographic expansion, the Steppe migration and a number of smaller population turnover events  
317 show clearly visible signals for most of our study regions.

318 An interesting result of our analysis concerns the role of outliers: In many described events of "massive"  
319 scale, the underlying signals are most visible in the presence of multiple individuals with very long origin-  
320 distances according to our algorithm. Indeed, we expect our mobility estimation to perform well in picking up  
321 outlier individuals who moved over a long distance in a short amount of time. The smaller the spatial distance  
322 of a mobility event and the longer the duration of the process, the more diffuse and unclear the respective  
323 signal gets, always highlighting pioneers over latecomers. But at the same time, we observe that there are  
324 many individuals with arguably more "local" genetic signatures. A possible prospect for future development  
325 would be to estimate fractions of migrants among groups, to gain a more nuanced understanding of how  
326 mobility affected communities. Significant shifts in local ancestry proportions can not only be the outcome  
327 of the often cited deliberate "mass migration", but potentially also of bottlenecks [Lin+16], forced migration  
328 [Mic+20], changes in reproductive behaviour [SP07], or the influence of a highly fertile minority [Bal+15].

329 To improve the results obtained in this paper, several important directions may be taken. Future research  
330 will probably be in a position to include more data as the sampling gaps in world wide ancient DNA data are  
331 quickly filled. That will make large-scale meta analysis more and more feasible and will allow for increased  
332 postdiction model resolution. Beyond that, developing more sophisticated spatiotemporal interpolation mod-  
333 els will be a core challenge. We are convinced that Gaussian process regression is a very powerful method,  
334 but maybe other approaches allow for more heterogeneous covariance settings dependent on the data density  
335 in space and time, or even involve full-scale machine-learning [BRK20]. One challenging aspect of an inter-  
336 polation through space and time, like in our method, is that it is not able to capture situations of multiple  
337 co-existing ancestries living in close proximity. Interpolation will in such cases create an average ancestry  
338 profile which may not be meaningful. Also for the mobility estimation method entirely different algorithms  
339 may be conceived, to get a more robust and precise measure compared to the one we present here. It may,  
340 for example, be possible to assign priors for the search of ancestry "origin" points and not follow genetic  
341 information blindly. This could include mobility information from artefact refitting [Clo00], isotope analy-  
342 sis [Bri20], least-cost-path calculation [VNG19] or genetic kinship analysis (e.g. [Mit+19]) – as derived by

343 archaeology or other neighbouring disciplines. Similarly, it may be possible to codify linguistic, historical or  
344 even archaeological data to derive alternative, quantitative large-scale measures of human mobility [RHS19].

## 345 **Materials and Methods**

346 All code for this paper with all relevant scripts and data is available in a repository here: <https://github.com/nevrome/mobest.analysis.2022> (an archived version with DOI will be added upon publication). From  
347 that we outsourced the main mobility estimation workflow into an R package available here: <https://github.com/nevrome/mobest>. All data analysis and plotting was done in R [R C21] with the following  
348 packages: Bchron [HP08], checkmate [Lan17], cowplot [Wil19], data.table [DS19], DiagrammeR [Ian20], fields  
349 [Dou+17], fractional [Ven16], future [Ben21], ggrepel [Slo21], ggridges [Wil21], igraph [CN06], khroma [Fre21],  
350 laGP [Gra16], latex2exp [Mes15], lemon [Edw20], raster [Hij21], rnatuarearth [Sou21], sf [Peb18], viridis  
351 [Gar+21] and finally the tidyverse and the many packages within it [Wic+19].  
352  
353

## 354 **Dataset**

355 Supplementary Table 1 summarises the dataset for this paper including the mean origin search output  
356 statistics. See Supplementary Tables for a description of the meaning of each variable/column. The raw input  
357 data was compiled from the Allen Ancient DNA Resource (AADR) v50 [Dav21] and modified with convertf  
358 [PPR06] and software tools from the genotype data management system Poseidon (<https://github.com/poseidon-framework>). We only included ancient DNA samples, and removed samples without spatial or  
359 temporal position information as well as samples outside of the defined research area (Fig. 2) and time  
360 window (median age within 8000calBC – 2000calAD).  
361

362 The dataset includes both samples whose DNA libraries have undergone in-solution enrichment capture  
363 as well as samples who have been sequenced evenly across the entire genome using the so-called shotgun  
364 approach. Each sample covers an individual subset of the 1240K SNP array [Mat+15]. For quality filtering  
365 we only kept samples with 25000 or more recovered autosomal SNPs on this array, determinable molecular  
366 sex and – for male individuals – an X-chromosome contamination value (determined with ANGSD [KAN14])  
367 smaller than 0.1. We also excluded samples that were explicitly marked as contaminated by the respective  
368 authors or assessed negatively in the AADR. In a final data filtering step we calculated pairwise distances  
369 (1 - proportion of alleles identical by state) among all samples and only kept the best preserved one from  
370 pairs/groups with distance values smaller 0.245, to remove closely related individuals or samples from the  
371 same individual.

372 All radiocarbon dates in the archaeological context data were recalibrated with the R package Bchron  
373 [HP08] (intercept calibration with IntCal20). Multiple radiocarbon dates for one sample were merged with  
374 sum calibration.

## 375 **Multidimensional scaling**

376 Multidimensional scaling is a dimensionality reduction method that can be applied to genetic data to derive  
377 positions in a genetic-distance space for individual samples. Before running it on our dataset with `plink`  
378 `--mdsplot v.1.9` [Pur+07] we removed SNPs in previously identified regions of high linkage disequilibrium  
379 within the 1240K SNP panel range according to Price et al. 2008 and Anderson et al. 2010 [Pri+08; And+10].

## 380 Gaussian process regression

381 Gaussian process regression is an interpolation method for n-dimensional space. The term *Gaussian process*  
382 means that a set of observations is modelled as the outcome of a multivariate normal distribution. Each  
383 observation can be described by its mean and a covariance matrix that encodes the relations among observa-  
384 tions. The method allows to make predictions for a dependent variable based on the position in independent  
385 variable space [Gra20]. It is a long-established method of geostatistics, where it is known as *kriging* [Mat63].  
386 Here we treat the position in spatial space (coordinates projected to EPSG:3035) and temporal space (years  
387 calBC/calAD randomly sampled from the post-calibration radiocarbon age or uniform archaeological context  
388 age probability distribution) as three independent variables that are used to predict the dependent position  
389 on each of two multidimensional scaling result dimensions. The prediction runs for a position grid that covers  
390 the land part of the research area (resolution: 100km, 50y) with some manually set, spatial masking of low  
391 data density regions (black in Figure 5).

392 A crucial step in the application of Gaussian process regression is the generation of a general covariance  
393 matrix with a sensible covariance function (*kernel*) that effectively describes the degree and range of long-  
394 distance effect the model assumes for individual observations. We followed the default choice for an *anisotropic*  
395 *Gaussian* kernel implemented in the R package laGP v.1.5-5 [Gra16]. laGP provides comparatively fast and  
396 accurate local approximate Gaussian process modelling [Hea+19]. The default laGP kernel has the form

$$\text{Cov}(x, x') = \tau^2 \exp \left( - \sum_{k=1}^p \frac{(x_k - x'_k)^2}{\theta_k} \right) + \eta_{x=x'}$$

397 with  $(x_k - x'_k)$  as the distance between all observations  $x$  and  $x'$  in the different dimensions  $k$  and the  
398 kernel size scaling factor  $\theta_k$  for each dimension.  $\eta_{x=x'}$  is the so called *nugget* term to account for different  
399 observations of the dependent variable at the same position in independent variable space.

400 The two values of  $\theta_k$  (spatial and temporal) and the value of  $\eta$  have to be fixed for the model, which  
401 is the second important decision necessary to define the covariance matrix. We applied multiple approaches  
402 (variogram analysis, maximum likelihood estimation, cross-validation) to estimate these parameters and  
403 present our results in Supplementary Text 1.

## 404 Mobility estimation algorithm and parameter exploration

405 For the mobility estimation or "origin search" performed with the interpolation grid we came up with a  
406 dedicated algorithm. For each individual in the selected analysis regions we searched for the genetically closest  
407 spatial position in a timeslice of the interpolation grid  $\approx 700$  years before their sampled age. Genetically closest  
408 means here: Has the least Euclidean distance in two dimensional MDS space. The "retrospection or rearview  
409 distance" was fixed based on the point of  $\text{Cov}(x, x') = 0.5$  on the temporal dimension. See Supplementary  
410 Text 2 for more details.

411 To explore the effect of 1. an MDS with three output dimensions and 2. different settings for the ret-  
412 rospection distance on the resulting regional mobility timeseries, we reran the analysis multiple times. See  
413 Supplementary Text 3 and the Supplementary Figures 1, 2 and 3 for the results with these modifications.

## 414 Acknowledgments

415 This research was financed by the International Max Planck Research School for the Science of Human  
416 History (IMPRS-SHH) and carried out on computational facilities of the Max Planck Institutes for the  
417 Science of Human History (MPI-SHH) and for Evolutionary Anthropology (MPI-EVA). Data collection  
418 was significantly simplified thanks to the Allen Ancient DNA Resource and the Poseidon genotype data  
419 initiative. We gratefully acknowledge insightful discussions with Joscha Gretzinger and helpful advice from  
420 Theseas C. Lamnidis, James A. Fellows Yates, He Yu, Ayshin Ghalichi, Ke Wang (all MPI-EVA), Martin Hinz  
421 (University Bern), Martin J. Kümmler (University Jena), Oliver Nakoinz (University Kiel) and all members  
422 of the Population genetics working group at the MPI-EVA.

## 423 References

- 424 [Al+19] Hussein Al-Asadi et al. “Estimating recent migration and population-size surfaces”. In: *PLoS*  
425 *Genetics* 15.1 (Jan. 2019). Ed. by Michael DeGiorgio, e1007908. DOI: 10.1371/journal.pgen.  
426 1007908.
- 427 [ALB18] Laura Alessandretti, Sune Lehmann, and Andrea Baronchelli. “Understanding the interplay  
428 between social and spatial behaviour”. In: *EPJ Data Science* 7.1 (Sept. 2018), p. 36.
- 429 [All+15] Morten E. Allentoft et al. “Population genomics of Bronze Age Eurasia”. In: *Nature* 522.7555  
430 (June 2015), pp. 167–172. DOI: 10.1038/nature14507.
- 431 [And+10] Carl A Anderson et al. “Data quality control in genetic case-control association studies”. In:  
432 *Nat. Protoc.* 5.9 (Aug. 2010), pp. 1564–1573. DOI: 10.1038/nprot.2010.116.
- 433 [Ant+19] Margaret L Antonio et al. “Ancient Rome: A genetic crossroads of Europe and the Mediter-  
434 ranean”. In: *Science* 366.6466 (Nov. 2019), pp. 708–714. ISSN: 0036-8075, 1095-9203. DOI: 10.  
435 1126/science.aay6826. URL: <http://dx.doi.org/10.1126/science.aay6826>.
- 436 [Ant90] David W Anthony. “Migration in Archeology: The Baby and the Bathwater”. In: *Am. Anthropol.*  
437 92.4 (1990), pp. 895–914.
- 438 [Bal+15] Patricia Balaesque et al. “Y-chromosome descent clusters and male differential reproductive  
439 success: young lineage expansions dominate Asian pastoral nomadic populations”. In: *Eur. J.*  
440 *Hum. Genet.* 23.10 (Oct. 2015), pp. 1413–1422. ISSN: 1018-4813, 1476-5438. DOI: 10.1038/  
441 ejhg.2014.285.
- 442 [Bar+18] Peter de Barros Damgaard et al. “137 ancient human genomes from across the Eurasian  
443 steppes”. In: *Nature* 557.7705 (May 2018), pp. 369–374. DOI: 10.1038/s41586-018-0094-2.
- 444 [Bel14] Peter Bellwood. *The Global Prehistory of Human Migration*. John Wiley & Sons, Nov. 2014.
- 445 [Ben01] Barbara Bender. “Landscapes on-the-move”. In: *Journal of Social Archaeology* 1.1 (June 2001),  
446 pp. 75–89. ISSN: 1469-6053. DOI: 10.1177/146960530100100106. URL: [https://doi.org/10.](https://doi.org/10.1177/146960530100100106)  
447 [1177/146960530100100106](https://doi.org/10.1177/146960530100100106).
- 448 [Ben21] Henrik Bengtsson. *A Unifying Framework for Parallel and Distributed Processing in R using*  
449 *Futures*. 10.32614/RJ-2021-048. 2021. URL: [https://journal.r-project.org/archive/  
450 2021/RJ-2021-048/index.html](https://journal.r-project.org/archive/2021/RJ-2021-048/index.html).

- 451 [Boc+09] Jean-Pierre Bocquet-Appel et al. “Detection of diffusion and contact zones of early farming in  
452 Europe from the space-time distribution of 14C dates”. In: *Journal of Archaeological Science*  
453 36.3 (Mar. 2009), pp. 807–820. DOI: 10.1016/j.jas.2008.11.004.
- 454 [Boc+12] Jean-Pierre Bocquet-Appel et al. “Understanding the rates of expansion of the farming system  
455 in Europe”. In: *J. Archaeol. Sci.* 39.2 (Feb. 2012), pp. 531–546. ISSN: 0305-4403. DOI: 10.1016/  
456 j.jas.2011.10.010.
- 457 [Boi+16] Nicole L Boivin et al. “Ecological consequences of human niche construction: Examining long-  
458 term anthropogenic shaping of global species distributions”. In: *Proc. Natl. Acad. Sci. U. S. A.*  
459 113.23 (June 2016), pp. 6388–6396.
- 460 [BR19] Gideon S. Bradburd and Peter L. Ralph. “Spatial Population Genetics: It’s About Time”. In:  
461 *Annual Review of Ecology, Evolution, and Systematics* 50.1 (Nov. 2019), pp. 427–449. DOI:  
462 10.1146/annurev-ecolsys-110316-022659.
- 463 [Bra+19] Selina Brace et al. “Ancient genomes indicate population replacement in Early Neolithic Britain”.  
464 In: *Nat Ecol Evol* 3.5 (May 2019), pp. 765–771. ISSN: 2397-334X. DOI: 10.1038/s41559-019-  
465 0871-9. URL: <http://dx.doi.org/10.1038/s41559-019-0871-9>.
- 466 [BRC16] Gideon S. Bradburd, Peter L. Ralph, and Graham M. Coop. “A Spatial Framework for Under-  
467 standing Population Structure and Admixture”. In: *PLOS Genetics* 12.1 (Jan. 2016). Ed. by  
468 Montgomery Slatkin, e1005703. DOI: 10.1371/journal.pgen.1005703.
- 469 [Bri20] Kate Britton. “Isotope Analysis for Mobility and Climate Studies”. In: *Archaeological Sci-  
470 ence: An Introduction*. Cambridge University Press, Jan. 2020, pp. 99–124. DOI: 10.1017/  
471 9781139013826.005.
- 472 [BRK20] C J Battey, Peter L Ralph, and Andrew D Kern. “Predicting geographic location from genetic  
473 variation with deep neural networks”. In: *eLife* 9 (June 2020). ISSN: 2050-084X. DOI: 10.7554/  
474 eLife.54507.
- 475 [Bru+20] Samantha Brunel et al. “Ancient genomes from present-day France unveil 7,000 years of its  
476 demographic history”. In: *Proc. Natl. Acad. Sci. U. S. A.* 117.23 (June 2020), pp. 12791–12798.  
477 ISSN: 0027-8424, 1091-6490. DOI: 10.1073/pnas.1918034117. URL: [http://dx.doi.org/10.](http://dx.doi.org/10.1073/pnas.1918034117)  
478 [1073/pnas.1918034117](http://dx.doi.org/10.1073/pnas.1918034117).
- 479 [Bur+20] Joachim Burger et al. “Low Prevalence of Lactase Persistence in Bronze Age Europe Indicates  
480 Ongoing Strong Selection over the Last 3,000 Years”. In: *Current Biology* 30.21 (Nov. 2020),  
481 4307–4315.e13. DOI: 10.1016/j.cub.2020.08.033.
- 482 [Bur00] Stefan Burmeister. “Archaeology and Migration: Approaches to an Archaeological Proof of  
483 Migration”. In: *Curr. Anthropol.* 41.4 (Aug. 2000), pp. 539–567.
- 484 [Cas+16] Lara M Cassidy et al. “Neolithic and Bronze Age migration to Ireland and establishment of the  
485 insular Atlantic genome”. In: *Proc. Natl. Acad. Sci. U. S. A.* 113.2 (Jan. 2016), pp. 368–373.  
486 ISSN: 0027-8424, 1091-6490. DOI: 10.1073/pnas.1518445113. URL: [http://dx.doi.org/10.](http://dx.doi.org/10.1073/pnas.1518445113)  
487 [1073/pnas.1518445113](http://dx.doi.org/10.1073/pnas.1518445113).
- 488 [Cas+20] Lara M Cassidy et al. “A dynastic elite in monumental Neolithic society”. In: *Nature* 582.7812  
489 (June 2020), pp. 384–388. ISSN: 0028-0836, 1476-4687. DOI: 10.1038/s41586-020-2378-6.  
490 URL: <http://dx.doi.org/10.1038/s41586-020-2378-6>.



- 491 [Clo00] Angela E Close. “Reconstructing Movement in Prehistory”. In: *Journal of Archaeological Method*  
492 *and Theory* 7.1 (2000), pp. 49–77. ISSN: 1573-7764. URL: [http://www.jstor.org/stable/](http://www.jstor.org/stable/20177412)  
493 20177412.
- 494 [CN06] Gabor Csardi and Tamas Nepusz. “The igraph software package for complex network research”.  
495 In: *InterJournal Complex Systems* (2006), p. 1695. URL: <https://igraph.org>.
- 496 [Dav21] David Reich Lab. *Allen Ancient DNA Resource (AADR): Downloadable genotypes of present-*  
497 *day and ancient DNA data, V50.0*. [https://reich.hms.harvard.edu/allen-ancient-dna-](https://reich.hms.harvard.edu/allen-ancient-dna-resource-aadr-downloadable-genotypes-present-day-and-ancient-dna-data)  
498 [resource-aadr-downloadable-genotypes-present-day-and-ancient-dna-data](https://reich.hms.harvard.edu/allen-ancient-dna-resource-aadr-downloadable-genotypes-present-day-and-ancient-dna-data). 2021.
- 499 [Dou+17] Douglas Nychka et al. *fields: Tools for spatial data*. R package version 12.5. Boulder, CO, USA:  
500 University Corporation for Atmospheric Research, 2017. DOI: 10.5065/D6W957CT. URL: [https:](https://github.com/NCAR/Fields)  
501 [//github.com/NCAR/Fields](https://github.com/NCAR/Fields).
- 502 [DS19] Matt Dowle and Arun Srinivasan. *data.table: Extension of ‘data.frame’*. R package version  
503 1.12.8. 2019. URL: <https://CRAN.R-project.org/package=data.table>.
- 504 [Edw20] Stefan McKinnon Edwards. *lemon: Freshing Up your ‘ggplot2’ Plots*. R package version 0.4.5.  
505 2020. URL: <https://CRAN.R-project.org/package=lemon>.
- 506 [Fer+18] D. M. Fernandes et al. “A genomic Neolithic time transect of hunter-farmer admixture in central  
507 Poland”. In: *Scientific Reports* 8.1 (Oct. 2018). DOI: 10.1038/s41598-018-33067-w.
- 508 [Fer+20] Daniel M. Fernandes et al. “The spread of steppe and Iranian-related ancestry in the islands  
509 of the western Mediterranean”. In: *Nature Ecology & Evolution* 4.3 (Feb. 2020), pp. 334–345.  
510 DOI: 10.1038/s41559-020-1102-0.
- 511 [Fis+18] Claire-Elise Fischer et al. “The multiple maternal legacy of the Late Iron Age group of Urville-  
512 Nacqueville (France, Normandy) documents a long-standing genetic contact zone in north-  
513 western France”. In: *PLoS One* 13.12 (Dec. 2018), e0207459. ISSN: 1932-6203. DOI: 10.1371/  
514 [journal.pone.0207459](http://dx.doi.org/10.1371/journal.pone.0207459). URL: <http://dx.doi.org/10.1371/journal.pone.0207459>.
- 515 [Fle+19] Pavel Flegontov et al. “Palaeo-Eskimo genetic ancestry and the peopling of Chukotka and North  
516 America”. In: *Nature* 570.7760 (June 2019), pp. 236–240.
- 517 [Fre+18] Rosa Fregel et al. “Ancient genomes from North Africa evidence prehistoric migrations to  
518 the Maghreb from both the Levant and Europe”. In: *Proceedings of the National Academy of*  
519 *Sciences of the United States of America* 115.26 (June 2018), pp. 6774–6779. ISSN: 0027-8424,  
520 1091-6490. DOI: 10.1073/pnas.1800851115.
- 521 [Fre21] Nicolas Frerebeau. *khroma: Colour Schemes for Scientific Data Visualization*. R package version  
522 1.7.0. Université Bordeaux Montaigne. Pessac, France, 2021. URL: [https://doi.org/10.5281/](https://doi.org/10.5281/zenodo.1472077)  
523 [zenodo.1472077](https://doi.org/10.5281/zenodo.1472077).
- 524 [Fur+20] Anja Furtwängler et al. “Ancient genomes reveal social and genetic structure of Late Neolithic  
525 Switzerland”. In: *Nat. Commun.* 11.1 (Apr. 2020), p. 1915. ISSN: 2041-1723. DOI: 10.1038/  
526 [s41467-020-15560-x](http://dx.doi.org/10.1038/s41467-020-15560-x). URL: <http://dx.doi.org/10.1038/s41467-020-15560-x>.
- 527 [Fur18] Martin Furholt. “Massive Migrations? The Impact of Recent aDNA Studies on our View of  
528 Third Millennium Europe”. In: *European Journal of Archaeology* 21.2 (May 2018), pp. 159–  
529 191.

- 530 [Fur21] Martin Furholt. “Mobility and Social Change: Understanding the European Neolithic Period  
531 after the Archaeogenetic Revolution”. In: *Journal of Archaeological Research* (Jan. 2021). DOI:  
532 10.1007/s10814-020-09153-x.
- 533 [Gar+21] Garnier et al. *viridis - Colorblind-Friendly Color Maps for R*. R package version 0.6.1. 2021.  
534 DOI: 10.5281/zenodo.4679424.
- 535 [GD15] Detlef Gronenborn and Pavel Dolukhanov. “Early Neolithic Manifestations in Central and East-  
536 ern Europe”. In: *The Oxford Handbook of Neolithic Europe*. Ed. by Chris Fowler, Jan Hard-  
537 ing, and Daniela Hofmann. Oxford University Press, Mar. 2015. DOI: 10.1093/oxfordhb/  
538 9780199545841.013.005.
- 539 [GF20] Omer Gokcumen and Michael Frachetti. “The Impact of Ancient Genome Studies in Archae-  
540 ology”. In: *Annual Review of Anthropology* 49.1 (2020), pp. 277–298. DOI: 10.1146/annurev-  
541 anthro-010220-074353.
- 542 [Gne+21] Guido Alberto Gnecci-Ruscione et al. “Ancient genomic time transect from the Central Asian  
543 Steppe unravels the history of the Scythians”. In: *Science Advances* 7.13 (Mar. 2021), eabe4414.  
544 DOI: 10.1126/sciadv.abe4414.
- 545 [Gon+17] Gloria González-Fortes et al. “Paleogenomic Evidence for Multi-generational Mixing between  
546 Neolithic Farmers and Mesolithic Hunter-Gatherers in the Lower Danube Basin”. In: *Current*  
547 *Biology* 27.12 (June 2017), 1801–1810.e10. DOI: 10.1016/j.cub.2017.05.023.
- 548 [Gon+19] G González-Fortes et al. “A western route of prehistoric human migration from Africa into  
549 the Iberian Peninsula”. In: *Proc. Biol. Sci.* 286.1895 (Jan. 2019), p. 20182288. ISSN: 0962-8452,  
550 1471-2954. DOI: 10.1098/rspb.2018.2288.
- 551 [Gra16] Robert B. Gramacy. “laGP: Large-Scale Spatial Modeling via Local Approximate Gaussian  
552 Processes in R”. In: *Journal of Statistical Software* 72.1 (2016), pp. 1–46. DOI: 10.18637/jss.  
553 v072.i01.
- 554 [Gra20] Robert B. Gramacy. *Surrogates: Gaussian Process Modeling, Design, and Optimization for the*  
555 *Applied Sciences*. Taylor & Francis Limited, 2020.
- 556 [Haa+10] Wolfgang Haak et al. “Ancient DNA from European Early Neolithic farmers reveals their Near  
557 Eastern affinities”. In: *PLoS biology* 8.11 (Nov. 2010), e1000536. ISSN: 1544-9173, 1545-7885.  
558 DOI: 10.1371/journal.pbio.1000536.
- 559 [Haa+15] Wolfgang Haak et al. “Massive migration from the steppe was a source for Indo-European  
560 languages in Europe”. In: *Nature* 522.7555 (June 2015), pp. 207–211.
- 561 [Hab+19] Marc Haber et al. “A Transient Pulse of Genetic Admixture from the Crusaders in the Near  
562 East Identified from Ancient Genome Sequences”. In: *Am. J. Hum. Genet.* 104.5 (May 2019),  
563 pp. 977–984. ISSN: 0002-9297, 1537-6605. DOI: 10.1016/j.ajhg.2019.03.015. URL: <http://dx.doi.org/10.1016/j.ajhg.2019.03.015>.
- 564
- 565 [Häg05] Torsten Hägerstrand. “What about people in regional science?” In: *Pap. Reg. Sci.* 24.1 (Jan.  
566 2005), pp. 7–24.
- 567 [Hea+19] Matthew J Heaton et al. “A Case Study Competition Among Methods for Analyzing Large  
568 Spatial Data”. In: *J. Agric. Biol. Environ. Stat.* 24.3 (2019), pp. 398–425.

- 569 [Hij21] Robert J. Hijmans. *raster: Geographic Data Analysis and Modeling*. R package version 3.4-13.  
570 2021. URL: <https://CRAN.R-project.org/package=raster>.
- 571 [Høg08] Henrik Høgh-Olesen. “Human Spatial Behaviour: The Spacing of People, Objects and Animals  
572 in Six Cross-Cultural Samples”. In: *J. Cogn. Cult.* 8.3-4 (Jan. 2008), pp. 245–280.
- 573 [HP08] John Haslett and Andrew C Parnell. “A simple monotone process with application to radiocarbon-  
574 dated depth chronologies”. In: *Journal of the Royal Statistical Society: Series C (Applied Statis-  
575 tics)* 57.4 (2008), pp. 399–418. DOI: 10.1111/j.1467-9876.2008.00623.x.
- 576 [Ian20] Richard Iannone. *DiagrammeR: Graph/Network Visualization*. R package version 1.0.6.1. 2020.  
577 URL: <https://CRAN.R-project.org/package=DiagrammeR>.
- 578 [Jär+19] Mari Järve et al. “Shifts in the Genetic Landscape of the Western Eurasian Steppe Associated  
579 with the Beginning and End of the Scythian Dominance”. In: *Curr. Biol.* 29.14 (July 2019),  
580 2430–2441.e10. ISSN: 0960-9822, 1879-0445. DOI: 10.1016/j.cub.2019.06.019. URL: <http://dx.doi.org/10.1016/j.cub.2019.06.019>.
- 582 [Jon+17] Eppie R Jones et al. “The Neolithic Transition in the Baltic Was Not Driven by Admixture  
583 with Early European Farmers”. In: *Curr. Biol.* 27.4 (Feb. 2017), pp. 576–582. ISSN: 0960-9822,  
584 1879-0445. DOI: 10.1016/j.cub.2016.12.060.
- 585 [KAN14] Thorfinn S. Korneliussen, Anders Albrechtsen, and Rasmus Nielsen. “ANGSD: Analysis of Next  
586 Generation Sequencing Data”. In: *BMC Bioinformatics* 15.1 (Nov. 2014), p. 356. ISSN: 1471-  
587 2105. DOI: 10.1186/s12859-014-0356-4.
- 588 [Kel92] Robert L Kelly. “Mobility/Sedentism: Concepts, Archaeological Measures, and Effects”. In:  
589 *Annu. Rev. Anthropol.* 21 (1992), pp. 43–66.
- 590 [KL05] Kristian Kristiansen and Thomas B. Larsson. *The Rise of Bronze Age Society - Travels, Trans-  
591 missions and Transformations*. Cambridge: Cambridge University Press, 2005. ISBN: 978-0-521-  
592 84363-8.
- 593 [Krz+18] Maja Krzewińska et al. “Ancient genomes suggest the eastern Pontic-Caspian steppe as the  
594 source of western Iron Age nomads”. In: *Science Advances* 4.10 (Oct. 2018), eaat4457. DOI:  
595 10.1126/sciadv.aat4457.
- 596 [Lan17] Michel Lang. “checkmate: Fast Argument Checks for Defensive R Programming”. In: *The R  
597 Journal* 9.1 (2017), pp. 437–445. URL: [https://journal.r-project.org/archive/2017/RJ-  
598 2017-028/index.html](https://journal.r-project.org/archive/2017/RJ-2017-028/index.html).
- 599 [Laz+14] Iosif Lazaridis et al. “Ancient human genomes suggest three ancestral populations for present-  
600 day Europeans”. In: *Nature* 513.7518 (Sept. 2014), pp. 409–413. ISSN: 0028-0836, 1476-4687.  
601 DOI: 10.1038/nature13673.
- 602 [Lin+16] John Lindo et al. “A time transect of exomes from a Native American population before and  
603 after European contact”. In: *Nat. Commun.* 7 (Nov. 2016), p. 13175. ISSN: 2041-1723. DOI:  
604 10.1038/ncomms13175.
- 605 [Lin+20] Anna Linderholm et al. “Corded Ware cultural complexity uncovered using genomic and isotopic  
606 analysis from south-eastern Poland”. In: *Sci. Rep.* 10.1 (Apr. 2020), p. 6885. ISSN: 2045-2322.  
607 DOI: 10.1038/s41598-020-63138-w. URL: [http://dx.doi.org/10.1038/s41598-020-  
608 63138-w](http://dx.doi.org/10.1038/s41598-020-63138-w).

- 609 [Lip+17] Mark Lipson et al. “Parallel palaeogenomic transects reveal complex genetic history of early  
610 European farmers”. In: *Nature* 551.7680 (Nov. 2017), pp. 368–372. DOI: 10.1038/nature24476.
- 611 [Lip+18] Mark Lipson et al. “Ancient genomes document multiple waves of migration in Southeast Asian  
612 prehistory”. In: *Science* 361.6397 (July 2018), pp. 92–95.
- 613 [LM15] Michelle A Lelièvre and Maureen E Marshall. “Because life it selfe is but motion’: Toward an  
614 anthropology of mobility”. In: *Anthropological Theory* 15.4 (Dec. 2015), pp. 434–471. ISSN: 1463-  
615 4996. DOI: 10.1177/1463499615605221. URL: <https://doi.org/10.1177/1463499615605221>.
- 616 [Loo+17] Liisa Loog et al. “Estimating mobility using sparse data: Application to human genetic varia-  
617 tion”. In: *Proc. Natl. Acad. Sci. U. S. A.* 114.46 (Nov. 2017), pp. 12213–12218.
- 618 [Mar+16] Rui Martiniano et al. “Genomic signals of migration and continuity in Britain before the  
619 Anglo-Saxons”. In: *Nat. Commun.* 7 (Jan. 2016), p. 10326. ISSN: 2041-1723. DOI: 10.1038/  
620 ncomms10326. URL: <http://dx.doi.org/10.1038/ncomms10326>.
- 621 [Mar+17] Rui Martiniano et al. “The population genomics of archaeological transition in west Iberia: In-  
622 vestigation of ancient substructure using imputation and haplotype-based methods”. In: *PLoS*  
623 *Genetics* 13.7 (July 2017). Ed. by Anna Di Rienzo, e1006852. DOI: 10.1371/journal.pgen.  
624 1006852.
- 625 [Mar+20a] Joseph H. Marcus et al. “Genetic history from the Middle Neolithic to present on the Mediter-  
626 ranean island of Sardinia”. In: *Nature Communications* 11.1 (Feb. 2020). DOI: 10.1038/s41467-  
627 020-14523-6.
- 628 [Mar+20b] Ashot Margaryan et al. “Population genomics of the Viking world”. In: *Nature* 585.7825 (Sept.  
629 2020), pp. 390–396. DOI: 10.1038/s41586-020-2688-8.
- 630 [Mat+15] Iain Mathieson et al. “Genome-wide patterns of selection in 230 ancient Eurasians”. In: *Nature*  
631 528.7583 (Dec. 2015), pp. 499–503. ISSN: 0028-0836, 1476-4687. DOI: 10.1038/nature16152.
- 632 [Mat+18] Iain Mathieson et al. “The genomic history of Southeastern Europe”. In: *Nature* 555.7695  
633 (Mar. 2018), pp. 197–203. ISSN: 0028-0836, 1476-4687. DOI: 10.1038/nature25778. URL: <http://dx.doi.org/10.1038/nature25778>.
- 634
- 635 [Mat63] Georges Matheron. “Principles of geostatistics”. In: *Econ. Geol.* 58.8 (Dec. 1963), pp. 1246–  
636 1266.
- 637 [Mes15] Stefano Meschiari. *latex2exp: Use LaTeX Expressions in Plots*. R package version 0.4.0. 2015.  
638 URL: <https://CRAN.R-project.org/package=latex2exp>.
- 639 [Mic+20] Steven J Micheletti et al. “Genetic Consequences of the Transatlantic Slave Trade in the Amer-  
640 icas”. In: *Am. J. Hum. Genet.* 107.2 (Aug. 2020), pp. 265–277. ISSN: 0002-9297, 1537-6605. DOI:  
641 10.1016/j.ajhg.2020.06.012. URL: <http://dx.doi.org/10.1016/j.ajhg.2020.06.012>.
- 642 [Mit+19] Alissa Mittnik et al. “Kinship-based social inequality in Bronze Age Europe”. In: *Science*  
643 366.6466 (Nov. 2019), pp. 731–734. ISSN: 0036-8075, 1095-9203. DOI: 10.1126/science.  
644 aax6219. URL: <http://dx.doi.org/10.1126/science.aax6219>.
- 645 [Nik+19] Alexey G Nikitin et al. “Interactions between earliest Linearbandkeramik farmers and Central  
646 European hunter gatherers at the dawn of European Neolithization”. In: *Sci. Rep.* 9.1 (Dec.  
647 2019), p. 19544. ISSN: 2045-2322. DOI: 10.1038/s41598-019-56029-2. URL: <http://dx.doi.org/10.1038/s41598-019-56029-2>.
- 648

- 649 [Ola+15] Iñigo Olalde et al. “A Common Genetic Origin for Early Farmers from Mediterranean Car-  
650 dial and Central European LBK Cultures”. In: *Molecular Biology and Evolution* (Sept. 2015),  
651 msv181. DOI: 10.1093/molbev/msv181.
- 652 [Ola+18] Iñigo Olalde et al. “The Beaker phenomenon and the genomic transformation of northwest  
653 Europe”. In: *Nature* 555.7695 (Mar. 2018), pp. 190–196. ISSN: 0028-0836, 1476-4687. DOI: 10.  
654 1038/nature25738. URL: <http://dx.doi.org/10.1038/nature25738>.
- 655 [Ola+19] Iñigo Olalde et al. “The genomic history of the Iberian Peninsula over the past 8000 years”.  
656 In: *Science* 363.6432 (Mar. 2019), pp. 1230–1234. ISSN: 0036-8075, 1095-9203. DOI: 10.1126/  
657 science.aav4040. URL: <http://dx.doi.org/10.1126/science.aav4040>.
- 658 [Pau19] B. Schulz Paulsson. “Radiocarbon dates and Bayesian modeling support maritime diffusion  
659 model for megaliths in Europe”. In: *Proceedings of the National Academy of Sciences* 116.9  
660 (Feb. 2019), pp. 3460–3465. DOI: 10.1073/pnas.1813268116.
- 661 [Peb18] Edzer Pebesma. “Simple Features for R: Standardized Support for Spatial Vector Data”. In:  
662 *The R Journal* 10.1 (2018), pp. 439–446. DOI: 10.32614/RJ-2018-009. URL: <https://doi.org/10.32614/RJ-2018-009>.
- 663
- 664 [Per+13] Camille Perchoux et al. “Conceptualization and measurement of environmental exposure in  
665 epidemiology: accounting for activity space related to daily mobility”. In: *Health Place* 21 (May  
666 2013), pp. 86–93.
- 667 [PNS15] Desislava Petkova, John Novembre, and Matthew Stephens. “Visualizing spatial population  
668 structure with estimated effective migration surfaces”. In: *Nature Genetics* 48.1 (Dec. 2015),  
669 pp. 94–100. DOI: 10.1038/ng.3464.
- 670 [Por+20] Marko Porčić et al. “The timing and tempo of the Neolithic expansion across the Central  
671 Balkans in the light of the new radiocarbon evidence”. In: *Journal of Archaeological Science:  
672 Reports* 33 (Oct. 2020), p. 102528. ISSN: 2352-409X. DOI: 10.1016/j.jasrep.2020.102528.
- 673 [PPN19] Benjamin M Peter, Desislava Petkova, and John Novembre. “Genetic Landscapes Reveal How  
674 Human Genetic Diversity Aligns with Geography”. In: *Molecular Biology and Evolution* 37.4  
675 (Nov. 2019). Ed. by Evelyne Heyer, pp. 943–951. DOI: 10.1093/molbev/msz280.
- 676 [PPR06] Nick Patterson, Alkes L. Price, and David Reich. “Population Structure and Eigenanalysis”.  
677 In: *PLoS Genetics* 2.12 (2006), e190. DOI: 10.1371/journal.pgen.0020190. URL: <https://doi.org/10.1371/journal.pgen.0020190>.
- 678
- 679 [Pri+08] Alkes L. Price et al. “Long-Range LD Can Confound Genome Scans in Admixed Populations”.  
680 In: *The American Journal of Human Genetics* 83.1 (2008), pp. 132–135. ISSN: 0002-9297. DOI:  
681 10.1016/j.ajhg.2008.06.005.
- 682 [Pur+07] Shaun Purcell et al. “PLINK: a tool set for whole-genome association and population-based  
683 linkage analyses”. In: *Am. J. Hum. Genet.* 81.3 (Sept. 2007), pp. 559–575.
- 684 [R C21] R Core Team. *R: A Language and Environment for Statistical Computing*. R Foundation for  
685 Statistical Computing. Vienna, Austria, 2021. URL: <https://www.R-project.org/>.
- 686 [Rac+20] Fernando Racimo et al. “The spatiotemporal spread of human migrations during the European  
687 Holocene”. In: *Proc. Natl. Acad. Sci. U. S. A.* 117.16 (Apr. 2020), pp. 8989–9000. ISSN: 0027-  
688 8424, 1091-6490. DOI: 10.1073/pnas.1920051117.

- 689 [RHS19] Felix Riede, Christian Hoggard, and Stephen Shennan. “Reconciling material cultures in ar-  
690 chaeology with genetic data requires robust cultural evolutionary taxonomies”. In: *Palgrave*  
691 *Communications* 5.1 (May 2019). DOI: 10.1057/s41599-019-0260-7.
- 692 [Riv+20] Maité Rivollat et al. “Ancient genome-wide DNA from France highlights the complexity of  
693 interactions between Mesolithic hunter-gatherers and Neolithic farmers”. In: *Sci Adv* 6.22 (May  
694 2020), eaaz5344. ISSN: 2375-2548. DOI: 10.1126/sciadv.aaz5344. URL: [http://dx.doi.org/  
695 10.1126/sciadv.aaz5344](http://dx.doi.org/10.1126/sciadv.aaz5344).
- 696 [Sán+19a] Federico Sánchez-Quinto et al. “Megalithic tombs in western and northern Neolithic Europe  
697 were linked to a kindred society”. In: *Proc. Natl. Acad. Sci. U. S. A.* 116.19 (May 2019),  
698 pp. 9469–9474. ISSN: 0027-8424, 1091-6490. DOI: 10.1073/pnas.1818037116. URL: [http://  
699 dx.doi.org/10.1073/pnas.1818037116](http://dx.doi.org/10.1073/pnas.1818037116).
- 700 [Sán+19b] Federico Sánchez-Quinto et al. “Megalithic tombs in western and northern Neolithic Europe  
701 were linked to a kindred society”. In: *Proceedings of the National Academy of Sciences* 116.19  
702 (Apr. 2019), pp. 9469–9474. DOI: 10.1073/pnas.1818037116.
- 703 [She10] J. A. Sheridan. “The Neolithisation of Britain and Ireland: the big picture”. In: *Landscapes in*  
704 *transition*. Ed. by B. Finlayson and G. Warren. Oxford: Oxbow Books, 2010, pp. 89–105.
- 705 [Sko+12] Pontus Skoglund et al. “Origins and genetic legacy of Neolithic farmers and hunter-gatherers  
706 in Europe”. In: *Science* 336.6080 (Apr. 2012), pp. 466–469. ISSN: 0036-8075.
- 707 [Slo21] Kamil Slowikowski. *ggrepel: Automatically Position Non-Overlapping Text Labels with 'ggplot2'*.  
708 R package version 0.9.1. 2021. URL: <https://CRAN.R-project.org/package=ggrepel>.
- 709 [Sou21] Andy South. *rnaturalearth: World Map Data from Natural Earth*. <https://docs.ropensci.org/rnaturalearth>  
710 (website) <https://github.com/ropensci/rnaturalearth>. 2021.
- 711 [SP07] Mark Q Sawyer and Tianna S Paschel. ““WE DIDN’T CROSS THE COLOR LINE, THE  
712 COLOR LINE CROSSED US”: Blackness and Immigration in the Dominican Republic, Puerto  
713 Rico, and the United States”. In: *Du Bois Rev.* 4.2 (2007), pp. 303–315. ISSN: 1742-058X,  
714 1742-0598. DOI: 10.1017/S1742058X07070178.
- 715 [Tho15] Nick Thorpe. “The Atlantic Mesolithic–Neolithic Transition”. In: *The Oxford Handbook of Ne-*  
716 *olithic Europe*. Ed. by Chris Fowler, Jan Harding, and Daniela Hofmann. Oxford University  
717 Press, Mar. 2015. ISBN: 9780199545841. DOI: 10.1093/oxfordhb/9780199545841.013.071.
- 718 [Val+18] Cristina Valdiosera et al. “Four millennia of Iberian biomolecular prehistory illustrate the im-  
719 pact of prehistoric migrations at the far end of Eurasia”. In: *Proceedings of the National Academy*  
720 *of Sciences* 115.13 (Mar. 2018), pp. 3428–3433. DOI: 10.1073/pnas.1717762115.
- 721 [Vee+18] Krishna R. Veeramah et al. “Population genomic analysis of elongated skulls reveals extensive  
722 female-biased immigration in Early Medieval Bavaria”. In: *Proceedings of the National Academy*  
723 *of Sciences* 115.13 (Mar. 2018), pp. 3494–3499. DOI: 10.1073/pnas.1719880115.
- 724 [Ven16] Bill Venables. *fractional: Vulgar Fractions in R*. R package version 0.1.3. 2016. URL: [https://  
725 CRAN.R-project.org/package=fractional](https://CRAN.R-project.org/package=fractional).

- 726 [VNG19] Philip Verhagen, Laure Nuninger, and Mark R Groenhuijzen. “Modelling of Pathways and  
727 Movement Networks in Archaeology: An Overview of Current Approaches”. In: *Finding the*  
728 *Limits of the Limes: Modelling Demography, Economy and Transport on the Edge of the Roman*  
729 *Empire*. Ed. by Philip Verhagen, Jamie Joyce, and Mark R Groenhuijzen. Cham: Springer  
730 International Publishing, 2019, pp. 217–249. ISBN: 9783030045760. DOI: 10.1007/978-3-030-  
731 04576-0\\_11.
- 732 [Wan+19] Chuan-Chao Wang et al. “Ancient human genome-wide data from a 3000-year interval in the  
733 Caucasus corresponds with eco-geographic regions”. In: *Nat. Commun.* 10.1 (Feb. 2019), p. 590.  
734 ISSN: 2041-1723. DOI: 10.1038/s41467-018-08220-8. URL: [http://dx.doi.org/10.1038/  
735 s41467-018-08220-8](http://dx.doi.org/10.1038/s41467-018-08220-8).
- 736 [Wic+19] Hadley Wickham et al. “Welcome to the tidyverse”. In: *Journal of Open Source Software* 4.43  
737 (2019), p. 1686. DOI: 10.21105/joss.01686.
- 738 [Wil19] Claus O. Wilke. *cowplot: Streamlined Plot Theme and Plot Annotations for 'ggplot2'*. R package  
739 version 1.0.0. 2019. URL: <https://CRAN.R-project.org/package=cowplot>.
- 740 [Wil21] Claus O. Wilke. *ggridges: Ridgeline Plots in 'ggplot2'*. R package version 0.5.3. 2021. URL:  
741 <https://CRAN.R-project.org/package=ggridges>.
- 742 [Wol19] Howard Wolinsky. “Ancient DNA and contemporary politics”. In: *EMBO reports* 20.12 (Nov.  
743 2019). DOI: 10.15252/embr.201949507.